Available online at www.sciencedirect.com

ScienceDirect

materialstoday: PROCEEDINGS

Materials Today: Proceedings 3 (2016) 780 – 787

12th International Conference on Nanosciences & Nanotechnologies & 8th International Symposium on Flexible Organic Electronics

Transmission of signals using white LEDs for VLC applications ☆

P. Louro[a,b]*, V. Silva[a,b], I. Rodrigues[a], M. A. Vieira[a,b], M. Vieira[a,b,b]

[1]*Electronics Telecommunication and Computer Dept,ISEL, R. Conselheiro Emídio Navarro 1 – 1959-007 Lisboa, Portugal*

[2]*CTS-UNINOVA, Universidade Nova de Lisboa), Quinta da Torre, Monte da Caparica, 2829-516, Caparica, Portugal*

[3]*DEE-FCT-UNL, Universidade Nova de Lisboa), Quinta da Torre, Monte da Caparica, 2829-516, Caparica, Portugal*

Abstract

In this paper an integrated wavelength optical filter and photodetector for Visible Light Communication (VLC) is used. The proposed application uses indoor warm light lamps lighting using ultra-bright white LEDs pulsed at frequencies higher than the ones perceived by the human eye. The system was analyzed using two different types the white LEDs, namely, phosphor and tri-chromatic based LEDs. The signals were transmitted into free space and the generated photocurrent was measured by the pin-pin photodetector based on a-SiC:H/a-Si:H. This device operates in the visible spectrum, allowing thus the detection of the pulsed white light emitted by the LEDs. However, as it also works as a visible optical filter with controlled wavelength sensitivity through the use of adequate optical biasing light, it is able to detect different wavelengths. This feature allows the detection of the individual components of the tri-chromatic white LED, which enlarges the amount of information transmitted by this type of white LED, when compared to the phosphor based LED. A capacitive optoelectronic model supports the experimental results and the physical operation of the device. A numerical simulation is presented.

Selection and peer-review under responsibility of the Conference Committee Members of NANOTEXNOLOGY2015
(12th International Conference on Nanosciences & Nanotechnologies & 8th International Symposium on Flexible Organic Electronics)

Keywords: amorphous SiC technology, optoelectronics, spectral sensitivity, white LEDs, visible light communication, numerical simulation

* Corresponding author. Tel.: +351919310252; fax: +351218317140.
E-mail address: plouro@deetc.isel.ipl.pt

2214-7853 © 2016 Published by Elsevier Ltd.
Selection and peer-review under responsibility of the Conference Committee Members of NANOTEXNOLOGY2015 (12th International Conference on Nanosciences & Nanotechnologies & 8th International Symposium on Flexible Organic Electronics)
doi:10.1016/j.matpr.2016.02.009

1. Introduction

Recent developments in LEDs allowed them to be used in environmental lighting and have revealed many advantages over incandescent light sources including lower energy consumption, longer lifetime, improved physical robustness, smaller size, and faster switching. Besides this general lighting application, LEDs are now used in other specific fields such as automotive headlamps, traffic signals, advertising, and camera flashes. However another emerging field of application is in advanced communications technology due to its high switching rates. Thus, the visible light spectrum is currently being used in the Visible Light Communication (VLC) technology, taking advantage of the lighting infrastructure based on white LEDs [1, 2, 3]. These energy-saving white light source devices were enabled by the invention of efficient blue LEDs, giving rise to two different technologies for the manufacture of white LEDs, either phosphor of tri-chromatic based LEDs [4].

In this paper we propose the use of a multilayered pin-pin device based on a-SiC:H [5, 6, 7] to work as a photo detector operating in the pertinent range of operation for VLC (375 nm – 780 nm) using as optical sources white LEDs. Optoelectronic characterization of the optical sources and of the photo detector show that the photo detector works as an optical filter in the visible range with tunable spectral sensitivity dependent on both applied bias and type of steady state optical bias (wavelength, intensity and direction of incidence on the device) [8]. A comparison of the performance of white LEDs phosphor based and tri-chromatic based is presented and discussed, demonstrating that the use of a tri-chromatic white LED enlarges the bandwidth of the visible communication system, when compared to the common, widely used phosphor based LEDs. A capacitive optoelectronic model supports the experimental results and explains the device operation.

2. Optoelectronic characterization

2.1. Optical sources

The proposed system compares the use of indoor lighting with ultra-bright white LEDs based on phosphor and using integrated tri-chromatic LEDs. The emission spectrum of each white LED was measured in the visible range using a commercial Czerny-Turner spectrometer. Obtained data are shown in Figure 1.

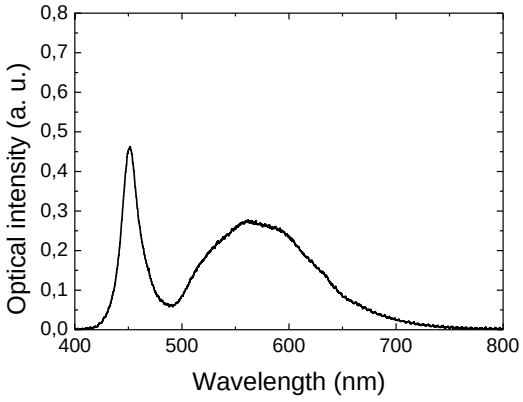

a)

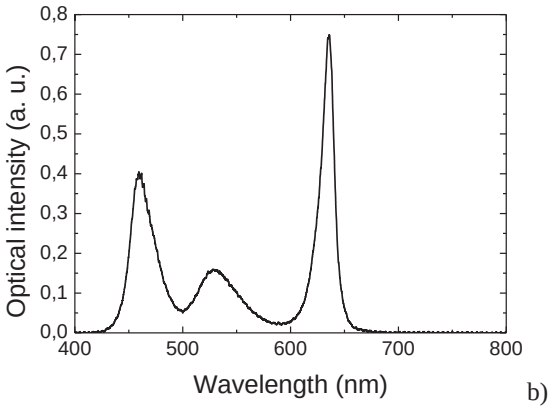

Fig. 1 Emission spectrum of the warm white LEDs: a) phosphor based; b) tri-chromatic based.

As expected, results show that the phosphor based white LED spectrum (Figure 1a) consists of one strong, sharp peak of short-wavelength blue light (at 452 nm) and a second, broader emission in the longer-wavelength part of the visible spectrum (centered at 570 nm and extending from 490 nm up to 700 nm). This is achieved by the absorption of the short wavelength light from the blue LED by the fluorescent phosphor layer that absorbs part of the blue light and re-emits light of a longer wavelength, which results in white light for the human eye perception. On the other hand, the spectrum of the tri-chromatic RGB white LED (Figure 1b) consists of three distinct peaks centered at the typical wavelengths of the red, green and blue colors of the visible spectrum, 635 nm, 532 nm and 463 nm, respectively. The perceived white light results from the additive mixing of the separate emitted wavelengths.

2.2. Photodetector device

Figure 2 shows the simplified cross-section structure of the device used to detect the transmitted information. It is a multilayer heterostructure composed by two pin structures (p-i'(a-SiC:H)-n/p-i(a-Si:H)-n) built on a glass substrate and sandwiched between two transparent electrical contacts [9, 10]. The front pin a-SiC:H photodiode is responsible for the device sensitivity in the short wavelengths of the visible range (400 - 550 nm) due to its minor thickness (200 nm) and higher band gap (2.1 eV). The back pin a-Si:H structure works in the complimentary part of the visible range, collecting the long wavelengths (520 - 700 nm) [11].

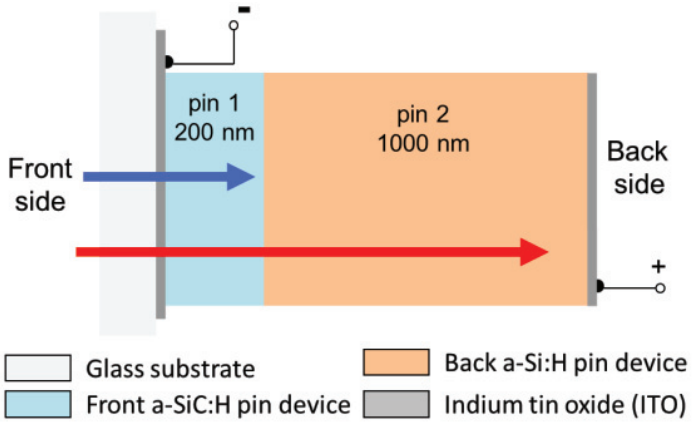

Fig. 2 Simplified schematic diagram of the device structure.

Figure 3 displays the photocurrent, measured along the visible spectrum, under reverse bias without and with optical

light bias focusing the device from back and front sides. Results show that the use of steady state light bias induces changes in the spectral sensitivity of the device. For long wavelengths (red at 600 nm) it is observed an amplification of the photocurrent under front optical bias while under optical bias from the back side the signal is reduced. For shorter wavelengths the opposite photocurrent behaviour is observed with a small amplification under back bias and a minor reduction under front bias.

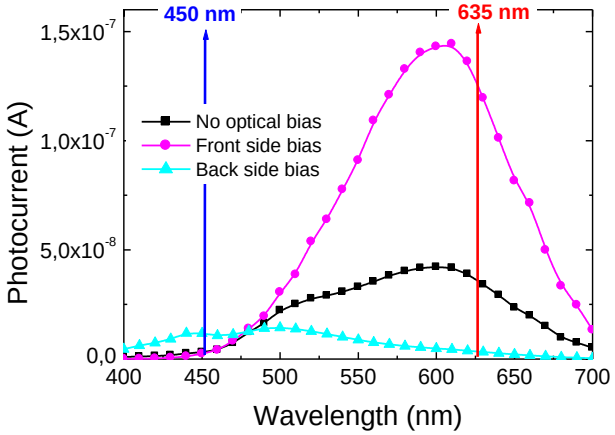

Fig. 3 Spectral photocurrent under dark conditions and using front and back violet light.

3. Transient analysis

3.1. White LEDs

The analysis of the system transient response was accomplished with the use of two white LEDs, pulsed at 1 kHz, with a square waveform driving current, in order to turn on and off the LEDs. The optical signals were transmitted in free space onto the device sensitive area (front side, Fig. 2). The driving current used to drive both LEDs was adjusted to generate the same output photocurrent signal. The tri-chromatic LED was modulated using for each internal LED (red, green and blue) the same driving current. Figure 4 shows the transient photocurrent measured under pulsed illumination of the white LEDs. On top of the figure the optical signal is displayed.

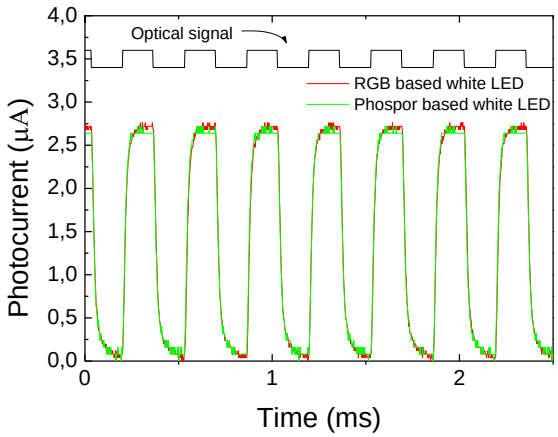

Fig. 4 Transient photocurrent measured under pulsed illumination of white LEDs.

Results show that the output signal follows the input optical signals driven by each LED, which allows for the decoding of the transmitted signal using an adequate receptor. In the case of a phosphor based white LED, there is

only one transmission channel that corresponds to the modulation of the internal blue LED. However, for the tri-chromatic LED, it is possible to control separately the signal applied and transmitted by each internal LED chip. This opens the possibility of transmitting simultaneously 3 optical channels, which extends considerably the bandwidth of the transmission system.

3.2. Tri-chromatic LED

In order to better characterize the white tri-chromatic LED, each internal chip was individually biased with the same driving current, and the optical signal illuminated the device from the front side. Optical bias was also used to soak uniformly the device separately from the front and back sides. A short wavelength was used (400 nm) and the optical intensity was adjusted to 0.630 mW/cm^2. Figure 5 shows the plot of the transient signals of the red and blue optical channels of the tri-chromatic white LED without and with violet front and back illumination. On top of the figure the optical signal is displayed.

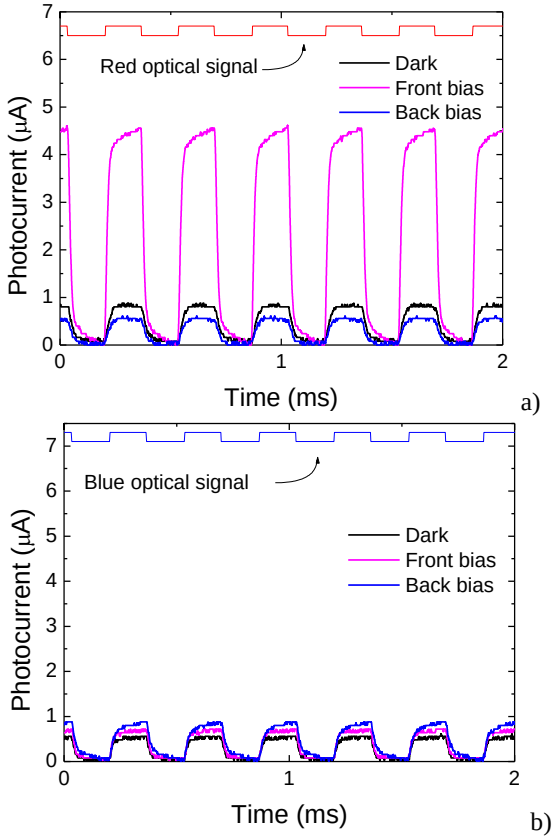

Fig. 5 Transient photocurrent measured under pulsed illumination of the internal LEDs of the tri-chromatic based white LED: a) red and b) blue internal LED, without optical bias and under front and back optical bias.

As expected from the spectral response data (Fig. 3) the red signal (Fig. 5a) is amplified under front bias and reduced under back bias, while nearly opposite behaviour is observed for the blue signal (Fig. 5b), since it is amplified using optical bias from the back side and remains nearly constant either with or without optical bias from the front side.

In order to analyse the photocurrent signal when the red and blue chips of the tri-chromatic white LED are transmitting a different signal, the internal LEDs were pulsed using different time dependent biasing currents. The output photocurrent signals measured under different optical bias conditions (with and without front and back

optical violet bias) are displayed in Figure 6. The condition assigned to all optical signals off corresponds to the reference level. The single optical signals are displayed at the top of the figure to help the reader with the different *on-off* optical states. The figure of merit used to quantify the signal amplification or attenuation is defined by the optical gain ($\alpha_{\lambda,F}$ and $\alpha_{\lambda,B}$ for the front and back gains, respectively), defined at each wavelength (λ) as the ratio between the signal magnitudes measured with and without optical bias.

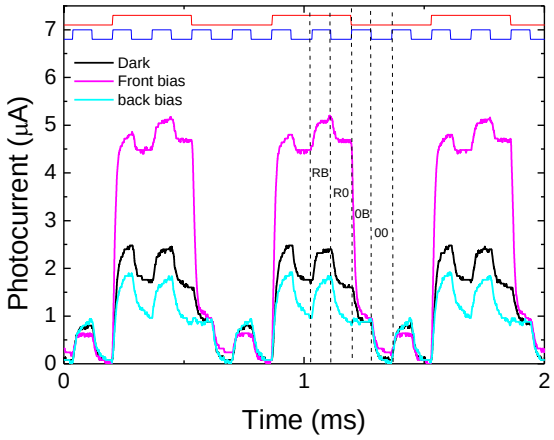

Fig. 6 Transient photocurrent measured under pulsed illumination of the tri-chromatic based white LED using different modulation currents for the red and blue internal LED chips, without optical bias and under front and back optical bias.

The photocurrent signal measured without optical bias (black line) exhibits four threshold levels that correspond to the four optical conditions of the input signals. The ON-ON (RB) state corresponds to the maximum intensity of light bias, while the ON-OFF (R0) and OFF-ON (0B) to a lower intensity and the OFF-OFF (00) to the dark conditions. However, when the device is optically biased the output photocurrent changes enhancing the presence of each input wavelength optical signal. Under front optical bias the output signal follows the shape of the red channel. Whenever the red optical signal is ON, the measured photocurrent is higher than its correspondent without optical bias. On the other hand, the use of optical bias at the device back side results in an output signal that follows the blue channel, which allows the recognition of the presence of this signal. Thus, the optical bias is able to tune the device sensitivity and to recognize the wavelength of the impinging light.

4. Decoding process

In the signal measured by the device front side (violet line in Fig. 6) the highest levels correspond to the presence of the red input channel, while the lowest ones to its absence. This mechanism allows the immediate recognition of the ON-OFF states for the red channel. Attending to the signal measured with violet illumination from the back side the same logic can be used (cyan lines in Fig. 6). Here the highest levels are assigned to the presence of the blue input signal when the red channel is on, which allows the immediate decoding of the blue channel. Thus, both red and blue channels can be immediately tuned by using adequate biasing light for the background.

The integration of the recovery information of each channel allows then the decoding of the whole data transmitted in the multiplexed signal. Using this simple key algorithm the independent red and blue bit sequences can be decoded, which demonstrates the ability of the device to interpret correctly each input optical signal. This features enables the possibility of duplicating the amount of information transmitted through the use of such tri-chromatic white LEDs in visible light communication.

5. Optoelectronic Model

Based on the experimental results and device configuration an optoelectronic model was developed.

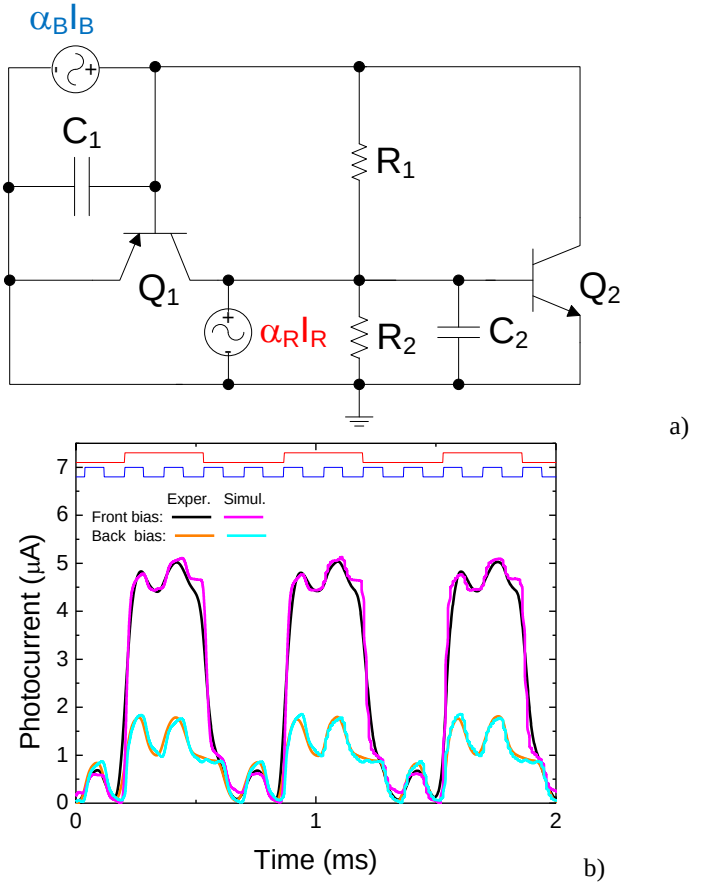

Fig 7 a) The ac equivalent circuit used for the optoelectronic model and b) results of a numerical simulation with front and back (□=400 nm) optical bias

The ac equivalent circuit used for the optoelectronic model (Fig. 7a) is based on amplifying elements (Q_1, Q_2), resistors (R_1, R_2) and capacitors (C_1, C_2). The proposed feedback loops adjust the desired filter characteristics with the experimental optical gains in the analyzed spectral region. The input signals, I_R and I_B, model the input channels. The amplifying elements, α_B and α_R are the optical gains of each impinging channel, respectively into the front and back phototransistors and provide gain ($\alpha>1$) or attenuate ($\alpha<1$) wavelengths.

A simple preprocessing denoising task was performed on the experimental photocurrents within the wavelets framework, under the assumption of non-Gaussian noise. The Haar wavelets were used to attain a five levels decomposition of the signals and the last two detail levels were removed by hard thresholding. A graphics user interface (GUI) computer program was designed and programmed within the MATLAB® programming language, to ease the task of numerical simulation. The linearized differential equation model was solved using the Runge-Kutta 4,5 method. To simulate the input channels we have used the individual magnitude of each input channel without background lighting, its bit sequence and the corresponding gain at the simulated background intensity.

Fig. 7b) presents results of a numerical simulation with front and back (λ=400 nm) optical bias, for the experimental data displayed in Fig. 6. A good agreement between experimental and simulated results was achieved for the photocurrents measured either using front or back optical bias. The adjustment parameters of the optoelectronic model were: C_1=0.8 nF, R_1=10kΩ, C_2(front)=0.2 nF, C_2(back) =0.15 nF R_2=1kΩ, $\alpha_{R,F}$ = 3.25, $\alpha_{R,B}$ = 0.5

Fig. 7 a) ac equivalent circuit of the optoelectronic device, b) Simulation and experimental data of the combined signal with front and back optical bias (C_1=0.8 nF, R_1=10kΩ, C_2 (front)=0.2 nF, C_2 (back)=0.15 nF R_2=1kΩ).0, $\alpha_{B,F}$ = 1.00, $\alpha_{B,B}$ = 1.10, I_R=0.36 mA and I_B=0.40 mA.0

6. Conclusions

A simple wireless communication system operating in free space within the visible spectrum was designed and its viability analyzed using different warm, white LEDs. System performance was evaluated using a phosphor based and a tri-chromatic white LEDs as optical sources and a double pin-pin heterostructure with two optical gate connections for light triggering in different spectral regions.

It was demonstrated the possibility of enlarging the amount of information transmitted in a VLC system using a tri-chromatic white LED instead of the cheaper phosphor based white LED. For this purpose, the need of an integrated photodetector and wavelength filter is a mandatory condition of the signal reception system. Spectral response characterization of the photodetector under different optical biasing conditions shows the dependence on the device absorption mechanism and supports the proposed algorithm to decode the input signal.

Future work comprises the analysis of the system in a wider range of optical fluxes, and the use of simultaneous transmission with the 3 LED chips available in the tri-chromatic based white LED. Further regulation of the individual driving currents of the internal LEDs of the tri-chromatic based white LED must also be exploited to improve the output current thresholds and enhance the decoding mechanism.

Acknowledgements

This work was supported by FCT (CTS multi annual funding) through the PIDDAC Program funds and PTDC/EEA-ELC/120539/2010.

[1] T. Komine, M. Nakagawa," Fundamental analysis for visible-light communication system using LED lights", IEEE Transactions on Consumer Electronics, Vol. 50, No. 1, FEB. 2004.

[2] PureVLC, Differences Between Radio & Visible Light Communications, PureVLC, 2012.

[3] S. Iwasaki, C. Premachandra, T. Endo, T. Fujii, M. Tanimoto, and Y. Kimura, "Visible light road-to-vehicle communication using high speed camera", IEEE Intelligent Vehicles Symposium, Eindhoven University of Technology, Eindhoven, The Netherlands, June 4-6, 2008.

[4] T. Komiyama, K. Kobayashi, K. Watanabe, T. Ohkubo, and Y. Kurihara, "Study of visible light communication system using RGB LED lights," in Proceedings of SICE Annual Conference, IEEE, 2011, pp. 1926–1928.

[5] M. Vieira, M. Fernandes, A. Fantoni, P. Louro, and R. Schwarz "A new CLSP sensor for Image recognition and color separation", Amorphous and Heterogeneous Silicon-Based Films-2002, Mat. Res. Soc. Symp. Proc., S. Francisco, April 1-5 U.S.A., Vol. 715 (2002) A4.3.

[6] P. Louro, M. Vieira, M. Fernandes, J. Costa, M. A. Vieira, J. Caeiro, N. Neves, M. Barata, "Optical demultiplexer based on na a-SiC:H voltage controlled device", Phys. Status Solidi C 7, No. 3–4, 1188– 1191 (2010) / DOI: 10.1002/pssc.200982702.

[7] P. Louro, M. Vieira, M. A. Vieira, S. Amaral, J. Costa, M. Fernandes, "Optical Demultiplexer Device Operating in the Visible Spectrum", Sensors & Actuators: A Physical vol. 172 (1), 35-39 (2011) http://dx.doi.org/10.1016/j.sna.2011.01.026.

[8] P. Louro, M. Vieira, M. A. Vieira, M. Fernandes and J. Costa (2011). "Use of a-SiC:H Photodiodes in Optical Communications Applications", Advances in Photodiodes, Gian Franco Dalla Betta (Ed.), ISBN: 978-953-307-163-3, InTech, Chap.19, pp:377-402 (2011).

[9] M. Vieira, P. Louro, M. A. Vieira, M. Fernandes, J. Costa, A. Fantoni, and M. A. Barata, "Optical processing devices based on a-SiC:H multilayer architectures", Phys. Status Solidi C 7, No. 3–4, 1184– 1187 (2010) / DOI: 10.1002/pssc.200982700.

[10] M. Vieira, M. Fernandes, P. Louro, R. Schwarz, M. Schubert, "Image capture devices based on p-i-n silicon carbides for biometrics applications", J. Non Cryst. Solids 299-302 (2002) pp. 1245-1249. DOI: 10.1016/S0022-3093(01)01145-0.